

Formation of surface dust vortex at mesoscale atmospheric depression

V.A. Shlychkov and V.M. Mal'bakhov

*Novosibirsk Affiliate of the Institute of Water and Ecological Problems,
Siberian Branch of the Russian Academy of Sciences
Institute of Computational Mathematics and Mathematical Geophysics,
Siberian Branch of the Russian Academy of Sciences, Novosibirsk*

Received January 31, 2001

A 3D model of mesoscale atmospheric dust vortices with a vertical axis of revolution is proposed. The mass of solid particles entrapped into the vortex from a sand-covered land surface is estimated.

Introduction

Observations show that dust vortices, whose axis of revolution is nearly vertical, often arise in summer above arid regions. The horizontal dimensions of these vortices rarely exceed 100 m, while the vertical dimensions are several times larger. The speed of vortices, as judged from the concentration of dust particles in them, can range from 10 to 30 m/s. The near-surface speed can be rather high and sufficient for the uplift of aerosol particles from the sand-covered surface. Aerosol spreads upward under the effect of an upward going jet with the speed no less than several meters per second.

Because of the high concentration of aerosol and significant altitudes reaching several hundreds of meters, large dust vortices are quite visible even from space. In many features, the dust vortices are close to sandstorms and tornadoes arising at a front passage. However, dust vortices often arise in arid regions, and their main energy sources are the processes resulting from dry atmospheric instability, rather than humid one, as in sandstorms and tornadoes.^{1,2} Therefore, dust vortices are observed more often than storms and tornadoes. Nevertheless, large dust vortices are a unique phenomenon. They provide fast transport of aerosol particles from the ground to high altitudes, where they can be transported to large distances, participating for a long time in the processes of formation of clouds and precipitation. It is unclear by now why non-rotating convective cells (thermics and convective jets) transform into mesoscale surface vortices.

Thus, according to Ref. 2, for the surface vortex to arise, horizontal rotation must exist in the lower troposphere. However, some investigators believe that convective vortices can arise under the effect of shift and rotation of a plane-parallel flow as well.^{3–5} There are a lot of theoretical studies, which confirm or rebut, to some or other degree, the above ideas on the mechanism of appearance of mesoscale vortices. These are largely simplified, most often axisymmetric,

models.^{2,6} Such models cannot take into account the whole set of conditions leading to formation of vortices. Besides, model axisymmetric vortices can prove hydrodynamically unstable when solving the problem in 3D, rather than 2D, formulation.

The aim of this paper is to study one of the possible mechanisms of appearance of mesoscale dust vortices and to estimate the amount of aerosol lifted to the atmosphere using a 3D vortex model. We assume that a mesoscale vortex arises near the surface because of a nondivergent vortex field caused by mesoscale tropospheric depression above the unstable layer. The causes for appearance of such vortices in the upper part of the convective layer were studied in Refs. 3–5, and we omit them in this consideration.

In this paper, it will be shown that the presence of a vortex at the top of the convective layer can cause its concentration in a relatively narrow zone in the lower surface layer. This process is accompanied by the appearance of significant values of the rotational, radial, and vertical components of wind velocity near the surface. Just this pattern of air motion is typical of dust vortices. To describe the dynamics of the convective boundary layer, we use the eddy-resolving model, in which the processes of penetrating convection are described with the use of the so-called Large Eddy Simulation (LES) method. With such an approach applied, the vortices with the scale larger than 50 m are reproduced based on nonhydrostatic equations of thermohydrodynamics, whereas smaller ones are parameterized. The sources of pollutants in the atmosphere are the processes of diffusion and saltation (wind-driven release of aerosol particles from the surface).

Spatial model of convective vortex

As the basic equations for describing the processes in the convective boundary layer, we take the equations of thermohydrodynamics that were used in Ref. 7 for modeling an ensemble of penetrating convection.

Denote the sought wind components in the Cartesian x, y, z coordinate system as u, v, w and write

$$\begin{aligned} \frac{du}{dt} &= -\frac{\partial \pi}{\partial x} + lv + D_{xy} u + \frac{\partial}{\partial z} K \frac{\partial u}{\partial z}, \\ \frac{dv}{dt} &= -\frac{\partial \pi}{\partial y} - lu + D_{xy} v + \frac{\partial}{\partial z} K \frac{\partial v}{\partial z}, \\ \frac{dw}{dt} &= -\frac{\partial \pi}{\partial z} + \lambda \theta + D_{xy} w + \frac{\partial}{\partial z} K \frac{\partial w}{\partial z}, \\ \frac{d\theta}{dt} + w \frac{\partial \theta}{\partial z} &= D_{xy} \theta + \frac{\partial}{\partial z} K_T \frac{\partial \theta}{\partial z}, \\ \frac{\partial u}{\partial x} + \frac{\partial v}{\partial y} + \frac{\partial w}{\partial z} &= 0, \end{aligned} \tag{1}$$

where θ is the convective deviation of the potential temperature from the background value $\Theta(z)$; K is the coefficient of vertical turbulent exchange of subgrid scale; $\frac{d}{dt} = \frac{\partial}{\partial t} + u \frac{\partial}{\partial x} + v \frac{\partial}{\partial y} + w \frac{\partial}{\partial z}$; $D_{xy} = \frac{\partial}{\partial x} K_x \frac{\partial}{\partial x} + \frac{\partial}{\partial y} K_y \frac{\partial}{\partial y}$ is the operator of horizontal turbulent exchange; λ is the buoyancy parameter; π is analog of pressure; l is the Coriolis parameter.²

As the conditions along the horizontal, we accept the assumption of periodicity. For the set of equations (1), the boundary conditions along the vertical are the following:

$$\begin{aligned} u = v = w = 0, \quad \theta = 0 \quad \text{at } z = 0, \\ u = u_H, \quad v = v_H, \quad \frac{\partial w}{\partial z} = 0, \quad \frac{\partial \theta}{\partial z} = 0 \quad \text{at } z = H, \end{aligned} \tag{2}$$

where $u_H(x, y)$ and $v_H(x, y)$ are determined from the equations $\frac{\partial u_H}{\partial x} + \frac{\partial v_H}{\partial y} = 0$ and $\frac{\partial v_H}{\partial x} - \frac{\partial u_H}{\partial y} = \omega_H$, ω_H is a given function characterizing the structure of a tropospheric vortex. The condition $\partial w / \partial z = 0$ at $z = H$ in this formulation has the meaning of conjugation of the surface vortex with the given tropospheric rotation. This condition is borrowed from Ref. 3, which studied the transmission of tropospheric rotation to cloud systems.

As the initial conditions, we take the absence of motion and temperature deviations at $t = 0$. The distribution of the background temperature is specified in the form of a compound function with 300-m-thick instability layer separated in the lower part and neutral stratification above this layer. The problem was solved in a $1 \times 1 \times 1$ km cube on the $64 \times 64 \times 200$ -node grid (in the $x, y,$ and z directions, respectively). The time step was equal to 1 s.

Let us specify the vorticity distribution on the upper boundary as an isolated perturbation with an extreme at the center of the zone ($x_0 = y_0 = 500$ m) as

$$\omega_H = 0.5 \exp(-\delta r^2),$$

where $r = \sqrt{(x - x_0)^2 + (y - y_0)^2}$ is the distance from the vortex axis; δ determines the rate of decrease of the vortex amplitude with the distance from its center (in our calculations $\delta = 10^{-4} \text{ m}^{-2}$). The velocity distribution is shown as a vector field in Fig. 1a.

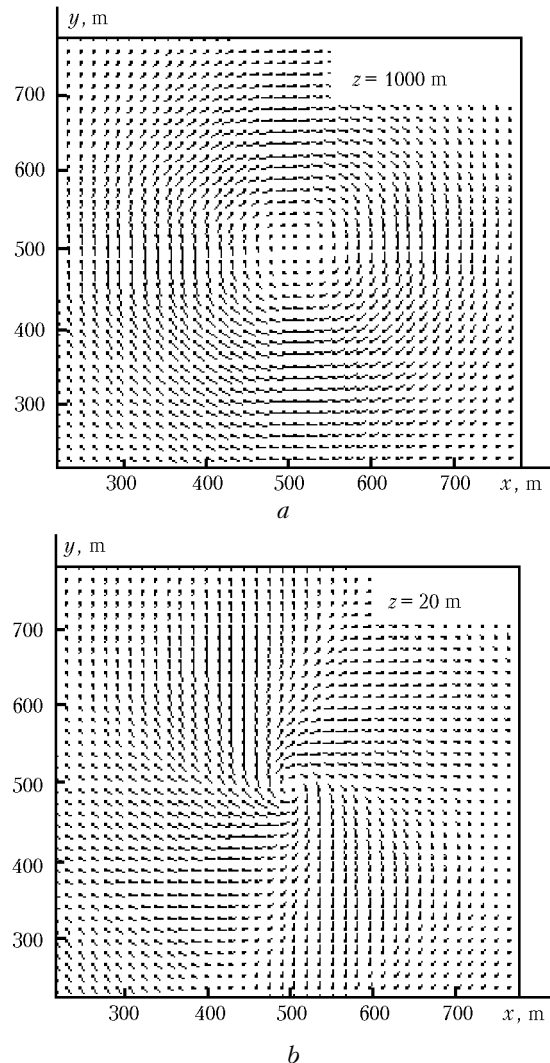


Fig. 1. Fragments of the velocity vector fields at the levels $z = H = 1000$ m (a) and $z = 20$ m (b).

The peak of the tangential speed v_n equal to 22 m/s is at the distance about 160 m from the center (the radial distribution of v_n is shown in Fig. 2a, curve 10).

Vorticity is transferred into the lower layers rather fast and has a nonmonotonic character. The vortex perturbation penetrates to the altitudes of 200–300 m roughly in 4 min of the model time due to the induced downward motions. The unstable stratification of the lower layer causes formation of a powerful thermic with the positive temperature deviations and the developed field of upward streams.

Moving downward, the angular momentum is transmitted to the “nonswirling” motion connected

with the purely coherent flow of air to the center near the surface. This causes rearrangement of the radial flow and appearance of the tangential component of velocity.

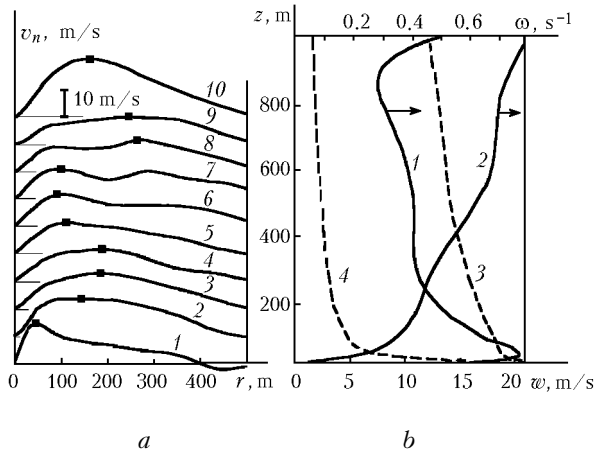


Fig. 2. Radial distribution of the tangential speed v_n at the levels $z = 10, 100, 200, \dots, 1000$ m (curves 1, 2, 3, ..., 10) (a); vertical profiles of ω , w , s (curves 1, 2, 3) at the vortex axis and the total value of s along the horizontal (curve 4) (b).

The mechanism of nonlinear advection and, possibly, the effect of large vertical shift of the wind near the ground at the speed about 12–15 m/s cause concentration of vorticity at the center up to the value of 0.78 s^{-1} , which exceeds the maximum value of the given vorticity field ω_H (0.5 s^{-1}) (see curve 1 in Fig. 2b drawn for $t = 12$ min). By that time, a rather stable pattern of the vortex-type flow has been formed; the characteristic feature of this pattern is pronounced localization of vorticity at the center of the region with an extreme near the surface. The extreme value increases with time.

According to the Helmholtz theorem, the strength of the vortex tube and, consequently, its radius are connected through an inverse relationship with the value of vorticity. It is seen from Fig. 2b that the vorticity decreases monotonically from the level $z = 0$ up to the altitudes of 800–900 m. Consequently, the size of the vortex tube increases with height, and the tube takes the conical shape.

As the centripetal motion increases, the amplitude of the orbital velocity in the lower part increases too. The maximum value of v_n is 15 m/s at the level $z = 20\text{--}30$ m near the vortex vertical axis. This can be seen from Fig. 2a, which shows the horizontal distribution of the tangential velocity at different levels (markers on the curves indicate the position of the maximum). The maximum of curve 1 corresponds to the level $z = 10$ m and is located 40 m far from the center, that is, the surface scale of the vortex is 80 m. Figure 1b illustrates the horizontal structure of the vortex near the surface. This pattern remains qualitatively unchanged for several minutes. Fifteen minutes after the beginning of integration, the vortex collapses as a result of the gradient catastrophe. The

axial revolution breaks with the formation of a series of perturbations with unclear geometry, which can be interpreted as a turbulent trace of an isolated vortex.

To describe spreading of a pollutant, let us use the equation

$$\frac{\partial s}{\partial t} + u \frac{\partial s}{\partial x} + v \frac{\partial s}{\partial y} + (w - w_0) \frac{\partial s}{\partial z} = D_{xy} s + \frac{\partial}{\partial z} K_S \frac{\partial s}{\partial z}, \quad (3)$$

where s is the pollutant concentration, $w_0(d)$ is the rate of gravitational sedimentation of particles with the diameter d .

The boundary conditions are formulated as

$$K_S \frac{\partial s}{\partial z} = -\Gamma \text{ at } z = 0; \quad \frac{\partial s}{\partial z} = 0 \text{ at } z = H,$$

where Γ is the intensity of a surface source of aerosol. The value of Γ was calculated by the technique proposed in Ref. 8; an example of testing the algorithm is given in Ref. 6.

As in Ref. 7, take $d = 125 \mu\text{m}$ and integrate Eq. (3) using the obtained fields of velocities and turbulence within the model (1) and (2). The calculations show that the surface wind speed needed for the particles' uplift is gathered for 7–8 min. The vertical profile of the concentration along the vortex axis is shown in Fig. 2b, curve 3. The curve is normalized to the maximum value of 8.8 g/m^3 . This concentration of fine aerosol in a volume of $10^6\text{--}10^7 \text{ m}^3$ attenuates several times the intensity of solar radiation, thus making the dust vortex quite visible.

The vertical speed in the vortex center (curve 2 in Fig. 2b) exceeds w_0 by an order of magnitude, therefore suspended particles entrapped into the turbulent flow are transported quickly to the upper layers, where the values of s are a little smaller than the surface ones (curve 3, Fig. 2b). On the vortex periphery, the intensity of vertical flows decreases and the most part of aerosol is deposited under the effect of gravity. The concentration profile changes its configuration, acquiring the characteristic "near-bottom" structure; the total distribution of s over x and y is shown as curve 4 in Fig. 2b (the maximum of the curve corresponds to the value of 110 t/m). The integral of this curve gives the total mass of the pollutant carried by the vortex. According to our calculations, this mass is 1350 t.

Thus, the results obtained suggest that the proposed model of the dust vortex is quite realistic.

The results of this work can be used to estimate the contribution of dust vortices to the supply of condensation and coagulation nuclei to the cloud layer. As is known, dust vortices can have an adverse effect, when they pass over the surface being a source of toxic aerosols. Nowadays, the drying Aral Sea is of a special hazard. In this region, dust vortices are frequent, and the wind-driven salt aerosol is transported to neighboring regions, deteriorating soil fertility in them. The proposed model in combination with the corresponding climatic and synoptic information can

help to solve the problem on the contribution of dust vortices to the process of transport of salt particles from the Aral Region.

Acknowledgments

The work was supported by the Russian Foundation for Basic Research, Grants No. 99–05–64735 and No. 99–05–64678.

References

1. L. Bengtsson and J. Lighthill, eds., *Intense Atmospheric Vortices* (Springer Verlag, Berlin, 1982).
2. L.N. Gutman, *Introduction to Nonlinear Theory of Mesometeorological Processes* (Gidrometeoizdat, Leningrad, 1969), 293 pp.
3. N.F. Vel'tishchev and R.B. Zaripov, *Izv. Ros. Akad. Nauk, Ser. Fiz. Atmos. Okeana* **36**, No. 2, 211–221 (2000).
4. D.K. Lilli, *J. Atmos. Sci.* **43**, No. 2, 113–126 (1986).
5. D.K. Lilli, *J. Atmos. Sci.* **43**, No. 2, 127–140 (1986).
6. V.M. Mal'bakhov and V.A. Shlychkov, *Atmos. Oceanic Opt.* **13**, No. 9, 818–820 (2000).
7. V.A. Shlychkov and P.Yu. Pushistov, in: *Bull. of the Novosibirsk Computing Center, Series "Numerical Modeling in the Atmosphere, Ocean and Environmental Studies"* (NCC Publisher, Novosibirsk, 2000), Application Issue 5, pp. 39–45.
8. E.K. Byutner, *Dynamics of the Near-Ground Air Layer* (Gidrometeoizdat, Leningrad, 1978), 157 pp.